One-dimensional Rashba states in Pb atomic chains on a semiconductor surface

A. N. Mihalyuk [1,2,*] J. P. Chou [3] S. V. Eremeev [4] A. V. Zotov [1] and A. A. Saranin [1]

[1]*Institute of Automation and Control Processes FEB RAS, 690041 Vladivostok, Russia*

[2]*School of Natural Sciences, Far Eastern Federal University, 690950 Vladivostok, Russia*

[3]*Department of Physics, National Changhua University of Education No. 1, Jinde Road, Changhua City, Changhua County 50007, Taiwan*

[4]*Institute of Strength Physics and Materials Science, Tomsk 634055, Russia*

(Received 16 May 2020; revised 10 July 2020; accepted 17 July 2020; published 30 July 2020)

We investigate the electronic and spin structure of Pb atomic chains on a Si(100)-2 × 1 surface using first-principles calculations. We revealed that the electronic spectra of linear dimerized Pb chains with orientations perpendicular and parallel to the Si dimers are characterized by one-dimensional large Rashba spin splitting providing exclusive spin polarization of the carriers that makes these systems suitable for studying the spin-transport phenomena and realizing a tunable spin current. A buckled dimerized Pb chain with a parallel orientation was predicted to be an insulating Rashba system with a vortical spin texture and asymmetric charge distribution. In this paper we trace the origin of Rashba band anisotropy and its interplay with chain geometry. The Rashba parameters of the considered chains are compared with other well-known systems.

DOI: 10.1103/PhysRevB.102.035442

I. INTRODUCTION

One-dimensional (1D) atomic scale chains on semiconductor surfaces are of increasing interest due to their unique quantum properties and potential applications in electronic devices. Along with practical applications, atomic chains are also the subject of interest from a fundamental point of view. Atomic thin chains are good examples to study the physics of low-dimensional systems and related intriguing phenomena, such as Peierls instability, which is a metal-insulator transition induced by charge density waves [1], nonconventional non-Fermi Luttinger-liquid behavior [2,3] when in 1D electron systems the Fermi-liquid approach is broken down [4], nontrivial topology [5], magnetism of nonmagnetic materials induced by unpaired spins of structural defects [6], and Shiba [7,8] and Majorana [9] states realized in a chain of magnetic atoms on the surface of a conventional 1D superconductor or *s*-wave superconductor, respectively.

Another actively studied phenomenon is a Rashba spin splitting [10] of the electronic states in a momentum space arising from spin-orbit coupling (SOC) and broken inversion symmetry at the surfaces and interfaces [11]. In particular, strong Rashba splitting was observed in 2D atomically thin films of metals with strong atomic SOC such as Bi [12], Tl [13], Sb [14], or Pt [15] adsorbed on silicon. It is known that lead has a number of phases in two dimensions and many outstanding properties. Apart from plumbene [16] on the Si(111) substrate, for example, 2D Pb may exist as a hexagonal incommensurate (HIC) phase [17] and as a striped incommensurate (SIC) phase [18]. Both Pb phases have Rashba spin-polarized states [19], and are known to be single-atomic-layer superconductors [20,21].

The Rashba-split states were also predicted and observed in a number of 1D systems, such as atomic chains [15,22] or edges of the surfaces [23]. In comparison with two- and three-dimensional systems, 1D Rashba materials are preferred since the 1D potential gradients can essentially be larger than those in the 2D or 3D systems because of the lower symmetry [24], as well as the SOC effect being greatly enhanced in reduced dimensions [25]. There is great interest in finding new electron structures that can generate pure spin currents [26] with a high efficiency and long spin diffusion lengths [27] among 1D systems. The important concern here is that spin-split bands should be metallic, which would allow enhanced spin transport [28].

The appropriate substrate supporting the nanowire is a crucial concern. The growth of 1D metallic systems may be realized on flat, stepped Si(111), Si(110), or high-index silicon surfaces Si(553) and Si(557) [29]. For example, Pt-induced nanowires on a Si(110) surface [15] present a well-ordered array whose spectrum is characterized by giant Rashba splitting and the presence of a 1D electron channel. Au chains on Si(553) and Si(557) substrates have metallic Rashba-split bands and present an ordered array of local magnetic moments or "spin chains" [30]. Rashba-split bands also were observed in Pb nanoribbons on a Si(553) vicinal surface [31]. However, other silicon substrates, such as Si(100)-2 × 1, are less investigated, though it can be a natural template facilitating 1D growth due to its Si dimer row structure.

Decades ago it was observed that the deposition of submonolayer Pb on a Si(100) surface leads to the formation of long quasi-one-dimensional Pb chains [32] oriented perpendicular to the underlying Si dimer rows and having a buckled geometry as confirmed by the total-energy calculations [33,34].

Recently, Pb atomic chains with various new geometries on the Si(100)-2 × 1 surface were grown and their atomic structures were comprehensively investigated by means of low-

*mih-alexey@yandex.ru

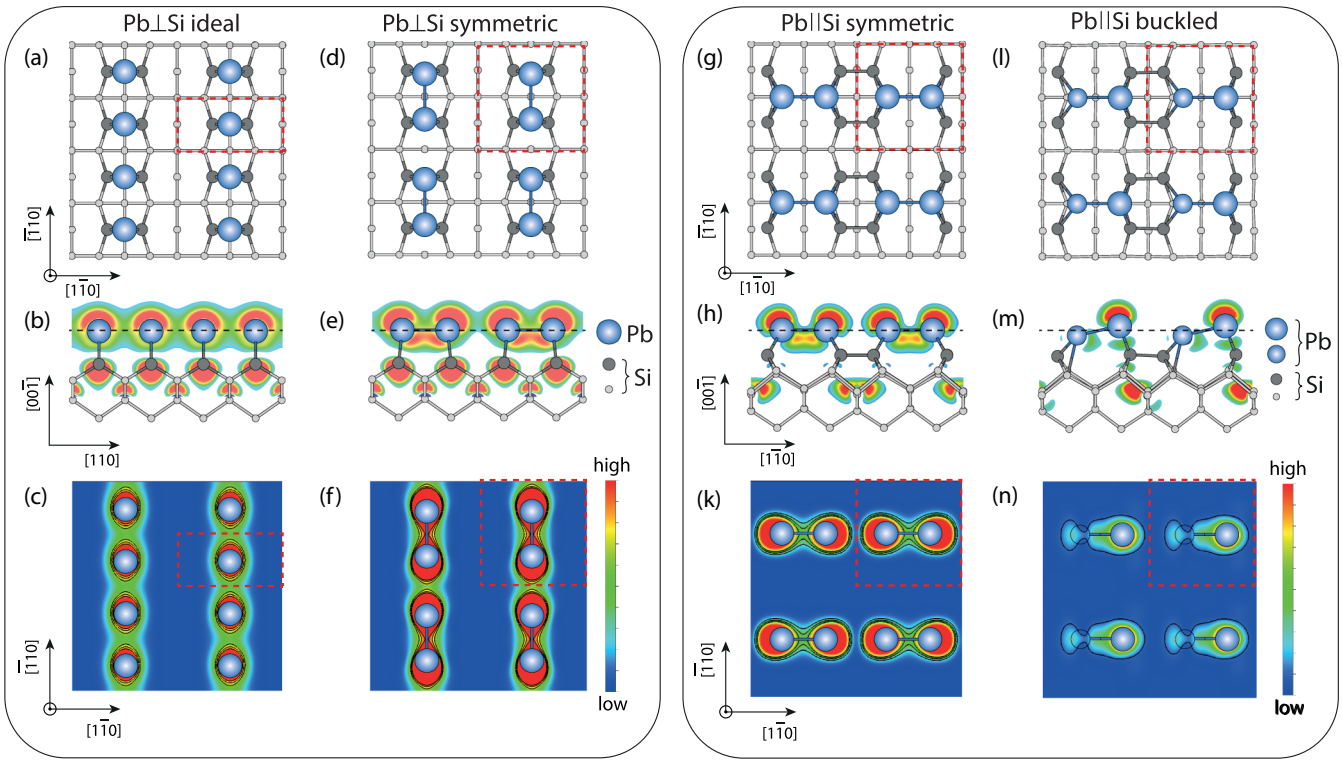

FIG. 1. Structural models of Pb chains on Si(100) and electron-density maps. (a) Ideal nondimerized hypothetical chain on the Si(100)-2 × 1 surface and (d) symmetric dimerized chain on Si(100)-2 × 2 on top and oriented perpendicular to the underlying Si dimers. (g) Symmetric and (l) buckled chains oriented parallel to the Si dimers and located in the trenches between the rows. Electron-density maps in side views [(b), (e), (h), (m)] and top views [(c), (f), (k), (n)] demonstrating the character of charge localization (Pb and Si atoms are superposed on the maps). Top view panels present the cuts of electron density made through the planes whose levels are shown by black dashed lines in the side view panels. Intensity color plot from blue to red is scaled from low to high charge density.

energy electron diffraction, scanning tunneling microscopy (STM), and total energy calculations [35]. Inspired by these results we undertake a theoretical study and predict several exotic electronic properties such as the presence of purely 1D Rashba bands with large spin splitting providing the ability for 1D spin-polarized electron transport.

II. CALCULATION DETAILS

We perform the density functional theory (DFT) calculations using the VASP code [36,37], with core electrons represented by projector augmented-wave (PAW) potentials [38]. The generalized gradient approximation of Perdew, Burke, and Ernzerhof (GGA-PBE) [39] to the exchange-correlation functional was employed for band structure calculations. The scalar relativistic effects and the spin-orbit coupling (SOC) were taken into account. To simulate the Pb chains on Si(100)-2 × 1 we used a slab consisting of 20 single layers (SLs) of silicon, at the PBE-optimized bulk Si lattice constant. Hydrogen atoms were used to passivate the Si dangling bonds at the bottom (unreconstructed) surface of the slab. The atomic positions of Pb atoms and atoms of Si layers within the six SLs of the slab were optimized. The silicon atoms of the deeper layers were kept fixed at the bulk crystalline positions. The geometry optimization was performed until the residual forces on the atoms were smaller than 10 meV/Å. The kinetic cutoff energy was 250 eV, and a 7 × 7 × 1 k-point mesh was used to sample the Brillouin zone (BZ). For getting an accurate Si band gap we apply the DFT-1/2 self-energy correction method [40,41] which only requires the addition of a self-energy correction potential, calculated from a half-ionized free atom, to the standard PAW-PBE potential of silicon. In order to verify the accuracy of the GGA-PBE approach for the description of the Pb p band dispersion we made additional calculations using the Heyd-Scuseria-Ernzerhof (HSE06) screened hybrid functional [42] for a free-standing Pb chain placed in a 2 × 1 unit cell of Si(100). A comparison of GGA-PBE and HSE06 spectra has shown that dispersions of Pb p states obtained within both methods are very similar [see Fig. 2(a)], especially in the vicinity of the Fermi level (±1 eV).

III. RESULTS AND DISCUSSION

A. Structural models

A pristine Si(100)-2 × 1 substrate has a natural 1D arrangement comprising a system of Si dimer rows and trenches going over the surface. This substrate geometry facilitates the subsequent formation of 1D atomic chains of adsorbed atoms. There are several ways to arrange Pb chains on a dimerized Si(100)-2 × 1 surface. First, the Pb chains might be oriented either parallel or perpendicular with respect to the underlying Si dimers. Then, Pb chains might be located either above the Si dimer rows, or in the trenches between them. Finally, the

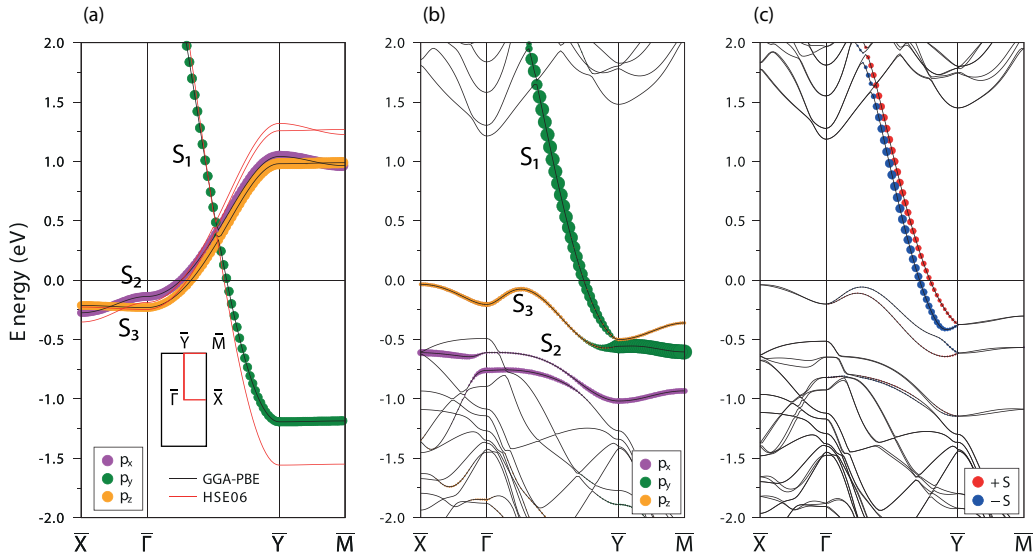

FIG. 2. Electronic structure of a Pb ⊥ Si ideal hypothetical chain in a 2 × 1 unit-cell. (a) Spectra of the free-standing chain calculated within GGA-PBE and HSE06 functionals (black and red lines, respectively). Orbital characters of the bands are shown by colored circles. The inset shows the Brillouin zone with high-symmetry points indicated. The spectrum of the Pb chain in the presence of a silicon substrate (b) without and (c) with spin-orbit coupling.

Pb chains might be either buckled (one Pb atom in a chain is higher than the other), or symmetric (all Pb atoms are at the same height). These all yield eight possible configurations. In the present study, we restricted our consideration to the three which were detected in STM experiments [35] demonstrating that these Pb chains are arranged as arrays of dimers. The most stable and abundant is the one with *buckled* Pb dimers residing *in trenches* and oriented *parallel* to Si dimers (to be denoted hereafter as Pb‖Si buckled) [Fig. 1(l)]. Sometimes in the middle of the long rows of Pb‖Si buckled chains, Pb dimers having a symmetric STM appearance were seen (to be denoted Pb‖Si symmetric) [Fig. 1(g)], which, according to calculations, are by 60 meV per 1 × 1 unit cell less stable. The other configuration having a close formation energy is the one with *symmetric* Pb dimers residing *above Si dimer rows* and oriented *perpendicular* to Si dimers (to be denoted hereafter as Pb ⊥ Si symmetric) [Fig. 1(d)]. STM observations have shown that this structure can occupy a considerable portion of the surface area, especially on the samples with a relatively high concentration of surface defects [35]. All other configurations were not observed in the STM experiments. Nevertheless, in order to trace the origin of the Rashba bands we would like to start with the idealized hypothetical structure with chains of nondimerized Pb atoms residing on top of the Si dimer rows and in the middle of Si dimers [Fig. 1(a)] as the most stable adsorption sites.

One of the important concerns is that the strength of the interaction between a substrate and atomic chain should be as weak as possible, otherwise the intrinsic electron properties of the chain will be suppressed due to the hybridization with electrons of the substrate. Let us now examine adsorption geometry and charge density distributions of the considered chains in order to estimate the strength of the Pb-Pb and Pb-Si interactions.

Each Pb atom in a Pb ⊥ Si ideal chain has two Pb-Si bonds with a bond length of 2.74 Å; Pb ⊥ Si and Pb‖Si symmetric chains have also two bonds (yielding 2.74 and 2.82 Å, respectively), while in the Pb‖Si buckled chain the upper Pb atom has also two bonds (equal to 2.87 Å), while the lower atom has three Pb-Si bonds, including one with a deeper silicon layer equal to 2.99 Å, that in general indicates a stronger Pb-Si interaction.

We calculated the electron-density maps obtained by the integration of charge density in the vicinity of the Fermi level, namely in the −50 to 0 meV range, and made their cuts along the chain direction [side view: Figs. 1(b), 1(e) 1(h), and 1(m)] and through the planes [top view: Figs. 1(c), 1(f) 1(k), and 1(n)] whose heights are shown by black dashed lines in the side view panels.

The electron-density maps of the Pb ⊥ Si ideal nondimerized chain [Figs. 1(b) and 1(c)] demonstrate the uniform charge distribution along the chain, while the density contours of the Pb ⊥ Si symmetric chain [Figs. 1(e) and 1(f)] have a shape of two connected charge clouds concentrated inside the Pb dimers with unclosed continuous intensities going through the whole unit cell along the chain direction, which indicates that electronic states near E_F in a symmetric chain have a mainly 1D character and are determined by the dominant Pb-Pb interactions.

The interconnection between charge clouds of a Pb‖Si symmetric chain is smaller and charge localization, in general, has a closed character with still pronounced anisotropy [Figs. 1(h) and 1(k)]. In all these chains the electron delocalization occurs along the chain direction but is strongly disfavored in the perpendicular direction, which is typical for the metallic chainlike structures on semiconductors with anisotropic band dispersion [30]. The overall appearance of the charge distribution of the Pb‖Si buckled chain demonstrates an isotropic character and a noticeable Pb-Pb charge asymmetry [Figs. 1(m) and 1(n)] when the charge cloud of the upper Pb atom is tiny and very loosely connected with a faint intensity spreading around the lower Pb atom. From the

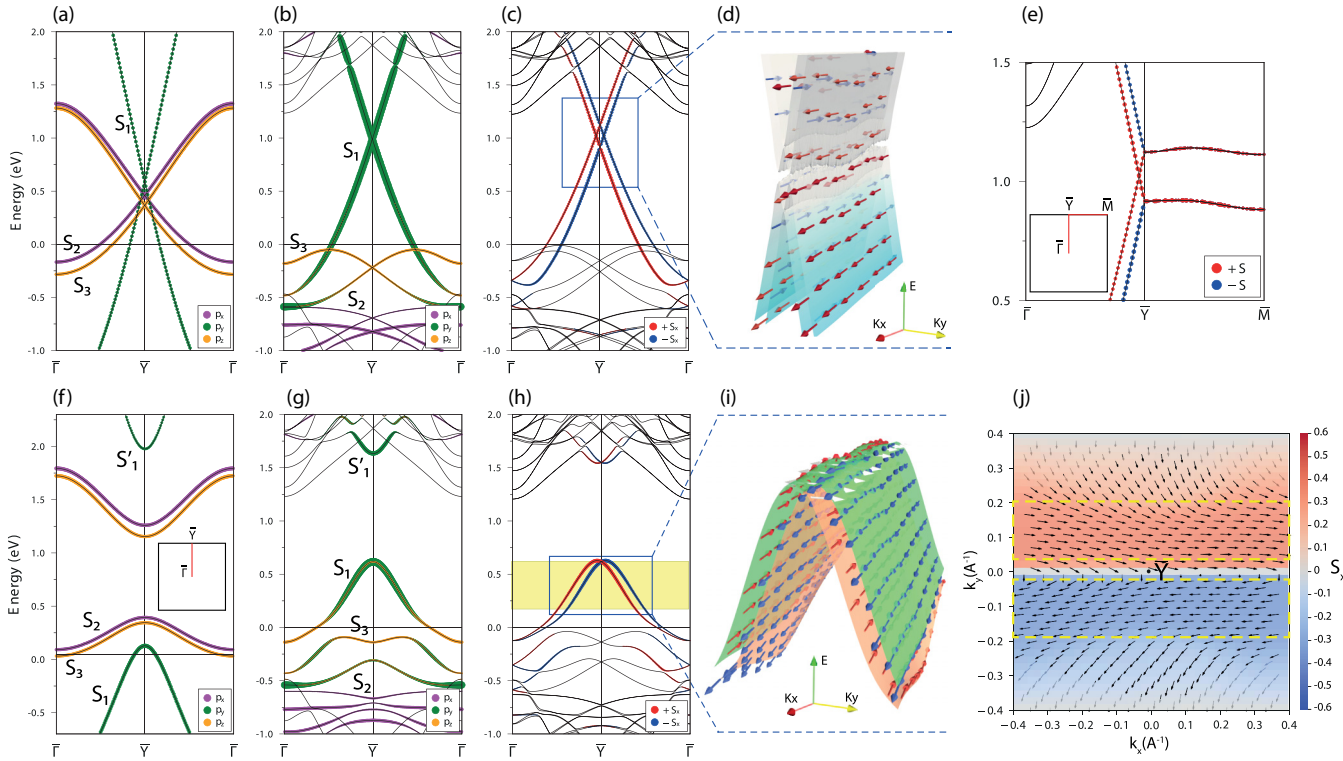

FIG. 3. Electronic structure of Pb ⊥ Si ideal hypothetical and Pb ⊥ Si symmetric dimerized chains in a 2 × 2 unit cell, displayed in the upper and lower panels, respectively. (a), (f) Free-standing case; (b), (g) and (c), (h) the substrate supported cases excluding and including spin-orbit coupling, respectively; (d), (i) enlarged volumetric view of the spin-split bands and associated spin texture with arrows representing the direction of spins; and (e) zoom with the spin-resolved spectrum along the $\bar{\Gamma}$-$\bar{Y}$-$\bar{M}$ direction. The inset shows the corresponding Brillouin zone with the indicated high-symmetry points. (j) $\bar{Y}$-centered plane projection of the spin texture for the outer Rashba band (the color intensity represents the absolute value of spin-orbit polarization). The yellow stripe in (h) and yellow dashed lines in (j) denote the 1D spin channel.

perspective of charge localization, this system appears as a quantum dot, rather than as a chain because of weak electron-density anisotropy, a strongly different charge localization at its two sites, and a missing interaction between neighboring Pb dimers.

B. Ideal hypothetical and symmetric dimerized Pb chains perpendicular to Si dimers

Before we examine the dimerized Pb ⊥ Si symmetric chain, let us consider the electronic structure of the ideal chain. The electronic spectrum of a hypothetical free-standing Pb chain placed in a Si(100)-2 × 1 unit cell [Fig. 2(a)] is characterized along the $\bar{\Gamma}$-$\bar{Y}$ direction (along the chain) by the intersection of a highly dispersing Pb p_y band (denoted as S1) with much heavier Pb p_x and p_z bands (denoted as S2 and S3, respectively). The Fermi velocity v_F of the S1 band is estimated to be 1.25×10^6 m/s, which is comparable with that for a graphene Dirac state varying from 0.85×10^6 to 1.73×10^6 m/s for a weak and strong electron-electron interaction, respectively [43].

The weak interchain interaction in the 2 × 1 cell leads to the emergence of a weak dispersion of the bands in the perpendicular direction, as well as causing a small lifting of the band degeneracy between the p_x and p_z bands, which is absent in the spectrum of the Pb chain with a wide vacuum spacing between chains (15 Å).

The spectrum of the ideal hypothetical Pb chain placed on the silicon substrate undergoes a number of changes, namely S2 and S3 bands (composed of Pb p_x and p_z orbitals, respectively) now are fully occupied and partially hybridized with a valence silicon band, as seen in the nonrelativistic spectrum in Fig. 2(b). The dispersion of the S1 band remains almost unchanged with the exception of a certain decreasing of its Fermi velocity down to $v_F = 0.71 \times 10^6$ m/s. In the presence of SOC the spectrum demonstrates a noticeable Rashba spin splitting along the chain with the Rashba parameter α_R yielding 1.29 eV Å for the S1 metallic band [Fig. 2(c)], where red and blue circles correspond to positive and negative S_x (perpendicular to the chain direction).

In order to compare the spectrum of a real dimerized Pb ⊥ Si symmetric chain with the spectrum of the ideal chain, we folded the initial band structure calculated at 2 × 1 BZ into 2 × 2 BZ. Figures 3(a)–3(c) demonstrate these results for the free-standing and substrate supported cases (excluding and including SOC). The spectrum of the dimerized Pb ⊥ Si symmetric chain undergoes the Peierls transition due to the dimerization of lead atoms. As a result, the initial Dirac-like bands, S1, S2, and S3, inherent in a Pb ⊥ Si ideal free-standing chain [Fig. 3(a)], transform to pairs of parabolic bands with a gap in between [Fig. 3(f)]. In the presence of the Si substrate, the upper and lower parabolic bands are merged into the conduction and valence silicon bands and only the S1 band remains metallic. In comparison with the Pb ⊥ Si ideal

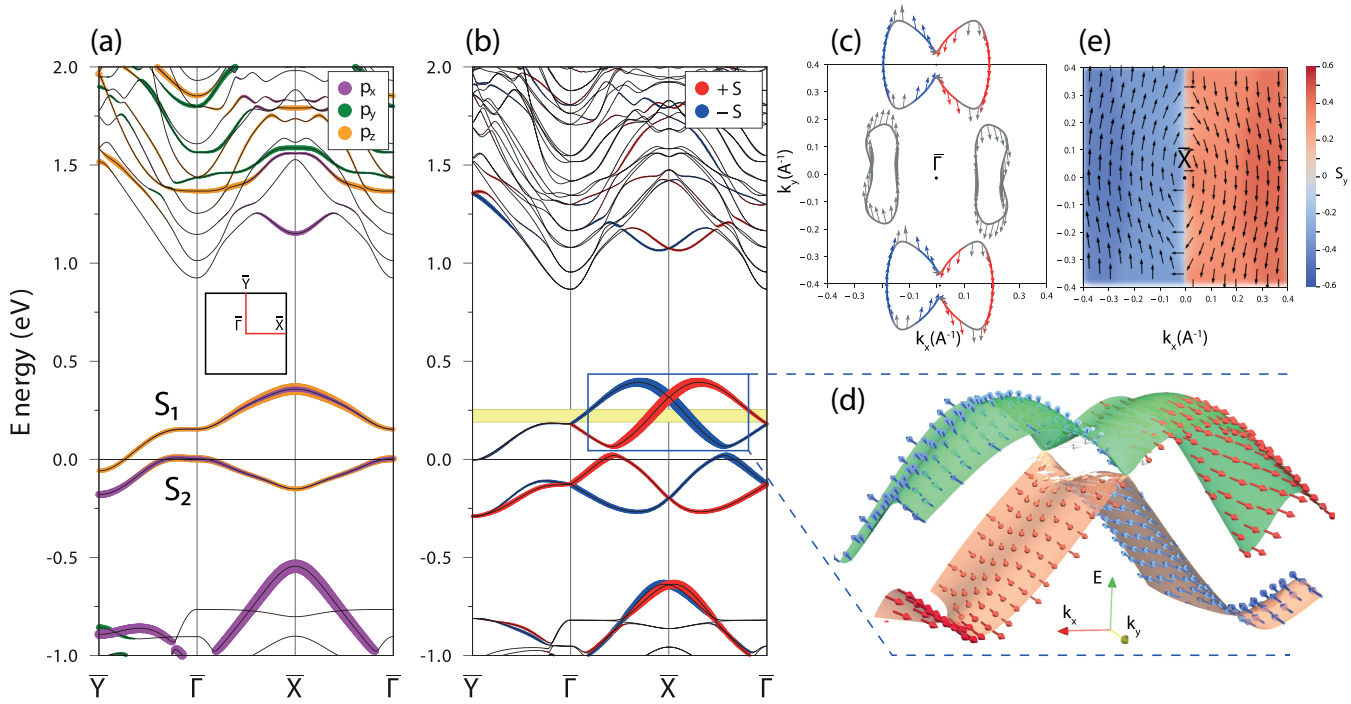

FIG. 4. Electronic structure of a Pb‖Si symmetric chain. (a) Orbital-projected nonrelativistic spectrum, with the inset showing the BZ with indicated high-symmetry points. (b) Spin-resolved spectrum, (c) its Fermi mapping, and (d) enlarged volumetric visualization of split bands and associated spin texture with arrows representing the direction of spins. (e) $\bar{X}$-centered plane projection of the spin structure of the outer branch of the Rashba-split S1 band. The yellow stripe in (b) denotes the 1D spin channel.

chain [Fig. 3(b)] now in the range from the Fermi level up to −0.5 eV, the strong hybridization between Pb p_y and p_z states is observed, while Pb p_x states are hybridized with the silicon valence band.

Let us again turn to the Pb ⊥ Si ideal chain and notice that in the presence of SOC the folded spectrum [Fig. 3(c)] demonstrates one new feature, namely a spin-split Dirac-like state at 1.05 eV above the Fermi level. The enlarged volumetric view of that crossing in Fig. 3(d) shows that the electronic system is characterized by a pure 1D spin texture and nodal line, which is more clearly shown in Fig. 3(e), demonstrating that in the $\bar{Y}$-$\bar{M}$ direction the bands are degenerate and almost dispersionless. In the case of the Pb ⊥ Si dimerized chain the SOC also lifts spin degeneracy and results in the appearance of the Rashba-split metallic S1 band [Fig. 3(h)].

The volumetric view of this state [Fig. 3(i)] displays the exclusive dominance of the S_x spin component and total absence of the S_z component. As one can see in the plane projection of the spin texture [Fig. 3(j)], the spin alignment has a completely 1D character in the k_y range of ± 0.2 Å^{-1} (around the $\bar{Y}$ point) that corresponds to the E range between 0.3 eV and the degeneracy point of the Rashba band [highlighted in Fig. 3(h) by a yellow stripe] where the S1 band is completely determined by p_y orbitals [see Fig. 3(g)]. Thus, achieving a purely 1D Rashba-split channel requires a tuning of the Fermi level into this energy range.

C. Symmetric Pb chain parallel to Si dimers

Let us examine the electronic properties of the Pb‖Si symmetric chain [Fig. 1(g)]. A nonrelativistic band structure calculation predicts two semimetallic bands, S1 and S2, which are composed of a mixture of Pb p_x and p_z orbitals, while Pb p_y states are fully hybridized with a silicon substrate and merged into the valence and conduction bands [Fig. 4(a)]. The large weight of the Pb p_z orbitals in the S1 and S2 bands reflects the strong Pb-Si interaction, though the interaction inside the Pb chain, determined by p_x states, is also observed in the system.

The relativistic spectrum in Fig. 4(b) shows that the band splitting primarily occurs along the chain axis corresponding to the $\bar{\Gamma}$-$\bar{X}$-$\bar{\Gamma}$ direction in the BZ and is characterized by large Rashba parameters α_R of 1.22 and 1.11 eV Å for the S1 and S2 bands, respectively, at the $\bar{X}$ point. In the orthogonal $\bar{\Gamma}$-$\bar{Y}$ direction there is also a certain band dispersion, though its spin splitting is vanishingly small. At the Fermi level there is a pair of hole pockets in the $\bar{\Gamma}$-$\bar{X}$-$\bar{\Gamma}$ direction and an electron pocket centered in the $\bar{Y}$ point. All Fermi contours demonstrate a nonvortical spin texture with a predominant S_y spin component as shown in Fig. 4(c). A similar spin structure was observed in the Tl monolayer on Si(110) which is a $C1_h$ system [44]. Remarkably, the hole pockets have identically zero S_z spin polarization (reflected by the gray color of the contours).

The volumetric visualization of the outer and inner branches of the Rashba-split S1 band and associated spin texture shown in Fig. 4(d) clearly demonstrates a mainly one-dimensional character of the spin alignment. The plane projection of spins for the outer branch of the S1 band in the whole BZ [Fig. 4(e)] supports the same evidence and reveals that the prevailing 1D spin orientation occurs in the vicinity of $\bar{\Gamma}$.

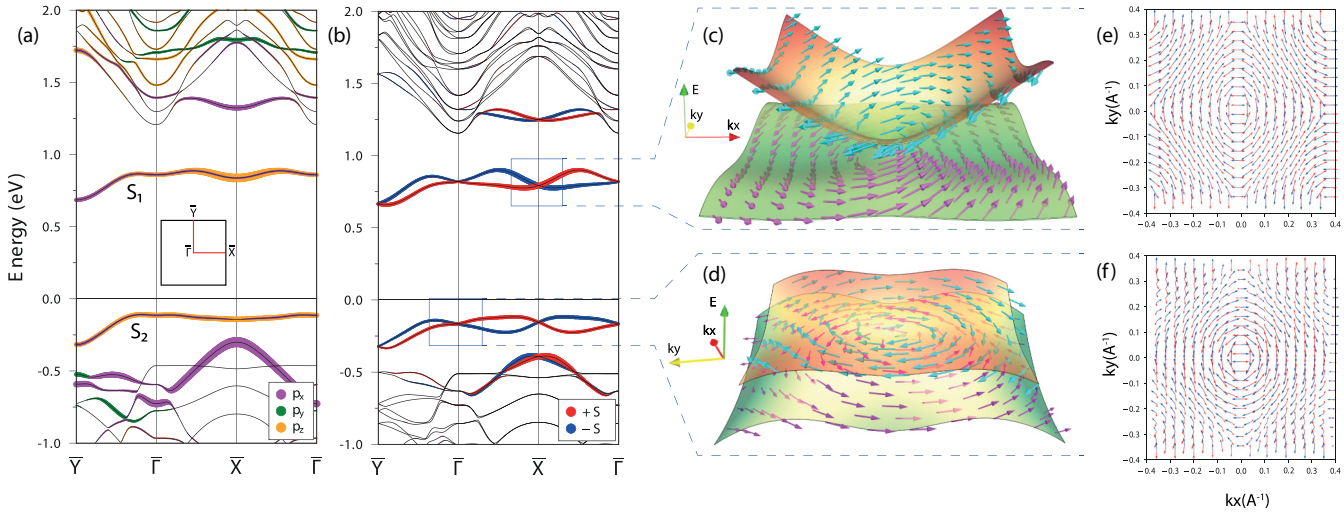

FIG. 5. Electronic structure of a Pb‖Si buckled chain. (a) Nonrelativistic and (b) spin-resolved spectra, where the inset shows BZ with high-symmetry points indicated. (c) and (d) Enlarged volumetric visualization of unoccupied and occupied bands, respectively, and (e), (f) their plane projections of the spin structure, where red and blue arrows correspond to the branches of the above-mentioned twofold degenerate bands.

Remarkably, in the spectrum there is a pure 1D spin channel with an exclusive S_y spin component [marked by the yellow stripe in Fig. 4(b)] if one could bring the Fermi level into the 0.18–0.25 eV range. Compared to the Pb ⊥ Si symmetric chain, in the current system the spin channel is of 70 meV width that is six times narrower, and also requires tuning of the Fermi level.

D. Buckled Pb chain parallel to Si dimers

According to the DFT calculations the band structure of the Pb‖Si buckled chain [Fig. 1(l)] reveals an insulating character of the system with two S1 and S2 weakly dispersing bands and a wide indirect gap yielding 790 meV [Fig. 5(a)]. The peculiarity of the chain is that the dispersion in the $\bar{\Gamma}$-$\bar{X}$ direction is almost absent, while in the $\bar{\Gamma}$-$\bar{Y}$ direction it is noticeable, thus indicating that the interchain interaction (mediated by a silicon substrate) is even more pronounced than the interaction inside the chain. Such a dispersion character, at a glance, is unexpected for the 1D atomic chain.

The orbital composition shows that both S1 and S2 bands are mainly filled with Pb p_z orbitals, pointing to the predominant Pb-Si interaction, while the weight of the p_x states related to the Pb-Pb interaction in these bands is weak. In comparison with the symmetric chain, the buckled geometry apparently suppresses the metallic character of the system.

In a relativistic spectrum [Fig. 5(b)] one may see the band splitting over the entire k space going in both orthogonal $\bar{\Gamma}$-$\bar{Y}$ and $\bar{\Gamma}$-$\bar{X}$ directions. An examination of the spin structure reveals vortex textures [Figs. 5(c) and 5(d)] instead of unidimensional ones, as again might being expected for a 1D system. The plain projections of the spin textures of the S1 and S2 bands demonstrate the presence of two helical centers in the spin-degenerate $\bar{X}$ [Fig. 5(e)] and $\bar{\Gamma}$ points [Fig. 5(f)], respectively. Their spin components follow behavior typical for Rashba helicity, namely the clockwise/counterclockwise spin rotation for the outer/inner Rashba branches.

Comparing the buckled and symmetric Pb‖Si chains and keeping in mind that both of them have a similar orientation, one may see that the symmetric geometry plays a crucial role in the emergence of 1D electronic anisotropy, as well as the strength of the Pb-Pb interaction.

IV. CONCLUSIONS

In summary, we performed a theoretical investigation of the electronic and spin structure of Pb chains with various geometries on a Si(100)-2 × 1 surface from first-principles calculations. Our study revealed that, depending on the chain geometry, its electronic spectrum may have a metallic, semimetallic, or insulating character. We have shown that Pb ⊥ Si and Pb‖Si symmetric chains behave as highly anisotropic materials providing metallic and semimetallic conductivity, respectively. The fine tuning of the Fermi level in these systems could allow for the realization of a purely 1D spin channel, which make these chains promising candidates for spintronics applications, and studying 1D Rashba state physics on semiconducting systems. Another fascinating finding for both symmetric chains is the large Rashba-type band splitting. Their Rashba parameters (>1 eV Å) belong to a few giant 1D Rashba systems (see Table I). For example, their Rashba parameters are an order of magnitude larger than those of semiconductor quantum wells (typically a few meV); they are larger than conventional 1D systems based on semiconductor quantum wire structures [47], or comparable with Pt nanowires on a Si(110) surface [15] as well of the same order as in a 2D Pb layer adsorbed on Ge(111) [28]. The Pb‖Si buckled chain has an insulating and weakly dispersing spectrum. The buckling character of the chain's array breaks the 1D arrangement of spins typical for chains with symmetric geometry and leads to the emergence of a vortical spin texture in both occupied and unoccupied Pb-derived Rashba bands. Thus, among the considered chains, the Pb ⊥ Si symmetric chain is the most promising for the realization of a

TABLE I. Selected Rashba systems and parameters characterizing the spin splitting of their bands: Rashba energy E_R (meV), momentum offset Δk_R (Å^{-1}), and Rashba parameter $\alpha_R = 2E_R/\Delta k_R$ (eV Å).

Materials	E_R	Δk_R	α_R
Bi/Ag(111) (2D) [45]	200	0.13	3.05
Pb/Ge(111) (2D) [28]	200	0.36	1.11
Pt/Si(110) nanowire (1D) [15]	81	0.12	1.36
Bi/InAs(110) (1D) [46]	290	0.105	5.5
BiIn/Si(111)-4 × 1 (1D) [24]	139	0.079	3.5
InGaAs/InAlAs interface (1D) [47]	<1	0.028	0.07
Pb/Si(100) Pb ⊥ Si symmetric (1D)	18	0.01	1.14
Pb/Si(100) Pb‖Si symmetric (1D)	69	0.125	1.11

unidirectional spin current in prospective applications since it has a wide 1D spin-polarized channel of 320 meV. It was revealed in recent STM experiments [35] that domains of Pb ⊥ Si symmetric chains can occupy a considerable portion of the surface area. We believe that our results may stimulate further studies of the exotic electronic phenomena in 1D or quasi-1D systems with spin-polarized electronic states as well as for the development of advanced spintronics applications.

ACKNOWLEDGMENTS

The DFT PBE calculations were supported by the Russian Science Foundation (Grant No. 19-12-00101). The HSE06 calculations were performed within the Fundamental Research Program of the State Academies of Sciences (line of research III.23.2.9). The calculations were conducted using the equipment of Shared Resource Center "Far Eastern Computing Resource" IACP FEB RAS [48].

[1] H. W. Yeom, S. Takeda, E. Rotenberg, I. Matsuda, K. Horikoshi, J. Schaefer, C. M. Lee, S. D. Kevan, T. Ohta, T. Nagao, and S. Hasegawa, Phys. Rev. Lett. **82**, 4898 (1999).
[2] O. M. Auslaender, A. Yacoby, R. de Picciotto, K. W. Baldwin, L. N. Pfeiffer, and K. W. West, Science **295**, 825 (2002).
[3] C. Blumenstein, J. Schäfer, S. Mietke, S. Meyer, A. Dollinger, M. Lochner, X. Y. Cui, L. Patthey, R. Matzdorf, and R. Claessen, Nat. Phys. **7**, 776 (2011).
[4] J. Voit, Rep. Prog. Phys. **58**, 977 (1995).
[5] S. Cheon, T.-H. Kim, S.-H. Lee, and H. W. Yeom, Science **350**, 182 (2015).
[6] S. C. Erwin and F. J. Himpsel, Nat. Commun. **1**, 58 (2010).
[7] S. Nadj-Perge, I. K. Drozdov, B. A. Bernevig, and A. Yazdani, Phys. Rev. B **88**, 020407(R) (2013).
[8] F. Pientka, L. I. Glazman, and F. von Oppen, Phys. Rev. B **88**, 155420 (2013).
[9] M. M. Maśka and T. Domański, Sci. Rep. **7**, 16193 (2017).
[10] Y. A. Bychkov and E. I. Rashba, Pis' ma Zh. Eksp. Teor. Fiz. **39**, 78 (1984).
[11] A. Manchon, H. C. Koo, J. Nitta, S. M. Frolov, and R. A. Duine, Nat. Mater. **14**, 871 (2015).
[12] E. Frantzeskakis, S. Pons, and M. Grioni, Phys. Rev. B **82**, 085440 (2010).
[13] S. D. Stolwijk, A. B. Schmidt, M. Donath, K. Sakamoto, and P. Krüger, Phys. Rev. Lett. **111**, 176402 (2013).
[14] X.-G. Zhu, Z. Liu, W. Li, J. Wen, X. Chen, J.-F. Jia, X.-C. Ma, K. He, L.-L. Wang, and Q.-K. Xue, Surf. Sci. **618**, 115 (2013).
[15] J. Park, S. W. Jung, M.-C. Jung, H. Yamane, N. Kosugi, and H. W. Yeom, Phys. Rev. Lett. **110**, 036801 (2013).
[16] J. Yuhara, B. He, N. Matsunami, M. Nakatake, and G. Le Lay, Adv. Mater. **31**, 1901017 (2019).
[17] S. Stepanovsky, M. Yakes, V. Yeh, M. Hupalo, and M. C. Tringides, Surf. Sci. **600**, 1417 (2006).
[18] M. Hupalo, J. Schmalian, and M. C. Tringides, Phys. Rev. Lett. **90**, 216106 (2003).
[19] J. H. Dil, F. Meier, J. Lobo-Checa, L. Patthey, G. Bihlmayer, and J. Osterwalder, Phys. Rev. Lett. **101**, 266802 (2008).
[20] T. Zhang, P. Cheng, W.-J. Li, Y.-J. Sun, G. Wang, X.-G. Zhu, K. He, L. Wang, X. Ma, X. Chen, Y. Wang, Y. Liu, H.-Q. Lin, J.-F. Jia, and Q.-K. Xue, Nat. Phys. **6**, 104 (2010).
[21] C. Brun, T. Cren, V. Cherkez, F. Debontridder, S. Pons, D. Fokin, M. C. Tringides, S. Bozhko, L. B. Ioffe, B. L. Altshuler, and D. Roditchev, Nat. Phys. **10**, 444 (2014).
[22] E. H. Do, S. G. Kwon, M. H. Kang, and H. W. Yeom, Sci. Rep. **8**, 15537 (2018).
[23] A. Takayama, T. Sato, S. Souma, T. Oguchi, and T. Takahashi, Phys. Rev. Lett. **114**, 066402 (2015).
[24] T. Tanaka and Y. Gohda, Phys. Rev. B **98**, 241409(R) (2018).
[25] A. Soumyanarayanan, N. Reyren, A. Fert, and C. Panagopoulos, Nature (London) **539**, 509 (2016).
[26] W. Han, S. Maekawa, and X.-C. Xie, Nat. Mater. **19**, 139 (2020).
[27] P. Song, C.-H. Hsu, G. Vignale, M. Zhao, J. Liu, Y. Deng, W. Fu, Y. Liu, Y. Zhang, H. Lin, V. M. Pereira, and K. P. Loh, Nat. Mater. **19**, 292 (2020).
[28] K. Yaji, Y. Ohtsubo, S. Hatta, H. Okuyama, K. Miyamoto, T. Okuda, A. Kimura, H. Namatame, M. Taniguchi, and T. Aruga, Nat. Commun. **1**, 17 (2010).
[29] P. C. Snijders and H. H. Weitering, Rev. Mod. Phys. **82**, 307 (2010).
[30] L. Dudy, J. Aulbach, T. Wagner, J. Schäfer, and R. Claessen, J. Phys.: Condens. Matter **29**, 433001 (2017).
[31] M. Kopciuszyński, M. Krawiec, R. Zdyb, and M. Jałochowski, Sci. Rep. **7**, 46215 (2017).
[32] J.-Y. Veuillen, J.-M. Gómez-Rodríguez, and R. C. Cinti, J. Vac. Sci. Technol. B **14**, 1010 (1996)
[33] M. E. González-Méndez and N. Takeuchi, Phys. Rev. B **58**, 16172 (1998).
[34] T.-L. Chan, C. Z. Wang, Z.-Y. Lu, and K. M. Ho, Phys. Rev. B **72**, 045405 (2005).
[35] V. Kotlyar, O. Utas, T. Utas, L. Bondarenko, A. Tupchaya, D. Gruznev, A. Mihalyuk, A. Zotov, and A. Saranin, Surf. Sci. **695**, 121574 (2020).
[36] G. Kresse and J. Hafner, Phys. Rev. B **47**, 558 (1993).

[37] G. Kresse and J. Furthmüller, Phys. Rev. B **54**, 11169 (1996).
[38] P. E. Blöchl, Phys. Rev. B **50**, 17953 (1994).
[39] J. P. Perdew, K. Burke, and M. Ernzerhof, Phys. Rev. Lett. **77**, 3865 (1996).
[40] L. G. Ferreira, M. Marques, and L. K. Teles, Phys. Rev. B **78**, 125116 (2008).
[41] L. G. Ferreira, M. Marques, and L. K. Teles, AIP Adv. **1**, 032119 (2011).
[42] A. V. Krukau, O. A. Vydrov, A. F. Izmaylov, and G. E. Scuseria, J. Chem. Phys. **125**, 224106 (2006).
[43] C. Hwang, D. A. Siegel, S.-K. Mo, W. Regan, A. Ismach, Y. Zhang, A. Zettl, and A. Lanzara, Sci. Rep. **2**, 590 (2012).
[44] E. Annese, T. Kuzumaki, B. Müller, Y. Yamamoto, H. Nakano, H. Kato, A. Araki, M. Ohtaka, T. Aoki, H. Ishikawa, T. Hayashida, J. R. Osiecki, K. Miyamoto, Y. Takeichi, A. Harasawa, K. Yaji, T. Shirasawa, K.-i. Nittoh, W. Yang, K. Miki, T. Oda, H. W. Yeom, and K. Sakamoto, Phys. Rev. Lett. **117**, 016803 (2016).
[45] C. R. Ast, J. Henk, A. Ernst, L. Moreschini, M. C. Falub, D. Pacilé, P. Bruno, K. Kern, and M. Grioni, Phys. Rev. Lett. **98**, 186807 (2007).
[46] T. Nakamura, Y. Ohtsubo, Y. Yamashita, S. I. Ideta, K. Tanaka, K. Yaji, A. Harasawa, S. Shin, F. Komori, R. Yukawa, K. Horiba, H. Kumigashira, and S. I. Kimura, Phys. Rev. B **98**, 075431 (2018).
[47] J. Nitta, T. Akazaki, H. Takayanagi, and T. Enoki, Phys. Rev. Lett. **78**, 1335 (1997).
[48] https://cc.dvo.ru.